Controlling the quantity of alpha-Fe inside multiwall carbon nanotubes filled with Fe-based crystals: The key role of vapor flow-rate

Boi, FS; Maugeri, S; Guo, J; Lan, M; Wang, S; Wen, J; Mountjoy, G; Baxendale, M; Nevill, G; Wilson, RM; He, Y; Zhang, S; Xiang, G

Controlling the quantity of α-Fe inside multiwall carbon nanotubes filled with Fe-based crystals: the key role of vapor flow-rate

Filippo S. Boi,[1,2,3,*] Serena Maugeri,[4] Jian Guo,[1,2,3] Gang Xiang,[1,2] Mu Lan,[1,2] Shanling Wang,[5] Jiqiu Wen,[5] Gavin Mountjoy,[6] Mark Baxendale,[4] George Nevill,[4] Rory M. Wilson,[7] Yi He,[5] and Sijie Zhang[1,2,3]

[1] *College of Physical Science and Technology, Sichuan University, 610064, Chengdu, China*
[2] *Key Laboratory of High Energy Density Physics and Technology of Ministry of Education, Sichuan University, Chengdu, 610064, China*
[3] *Sino-British Joint Materials Research Institute, Sichuan University, Chengdu 610064, China*
[4] *School of Physics and Astronomy, Queen Mary University of London, Mile End Road, London, E1 4NS, United Kingdom*
[5] *Analytical and Testing Center, Sichuan University, Chengdu, 610064, China*
[6] *School of Physical Sciences, University of Kent, Canterbury, CT2 7NH, United Kingdom*
[7] *School of Engineering and Materials Science, Queen Mary University of London, Mile End Road, London, E1 4NS, United Kingdom*

(Dated: September 2014)

The growth control of α-Fe inside multiwall carbon nanotubes has challenged researchers for more than a decade owing to the coexistence of this phase with Fe_3C and γ-Fe. Previously long heating treatments of 20 h has been used to decompose the encapsulated Fe-phases in C and Fe, however these methods were limited by an unusual oxidation process leading to nanotube decomposition. In this letter we report a novel chemical vapour deposition approach that through an accurate control of the ferrocene-vapour flow-rate allows to achieve the direct encapsulation of 95% of α-Fe without additional heating treatments.

In the last decade multiwall carbon nanotubes (MWCNTs) filled with α-Fe and iron-carbide Fe_3C single crystals have attracted the attention of numerous research groups [1–15] owing to their highly tunable magnetic properties. In particular large coercities of 0.160-0.180 Tesla [7] and exstremely high saturation magnetizations of 80 emu/g [5, 7, 8] have been achieved. The large coercivities of Fe_3C and α-Fe single crystals are very attractive for application in magnetic data storage, exchange bias systems, spin transport electronics, and other devices [1–11, 16–24]. However the coexistence of α-Fe with Fe_3C and γ-Fe crystals has limited the achievement of a complete control of their magnetic properties [1–12, 16–24].

In order to control the quantity of Fe_3C Heresanu *et al*. [6] suggested the use of fast cooling rates to "freeze" the Fe_3C crystals inside the MWCNTs. Instead, to maximize the quantity of α-Fe, a post-synthesis heating-treatment has been frequently considered since bulk γ-Fe can decompose into α-Fe and Fe_3C below 727 °C in a process involving the 9% of volume expansion [24–27]. Furthermore bulk Fe_3C can decompose into α-Fe and graphitic carbon when in contact with graphite (MWCNTs walls) in the temperature range of 500-550 °C [27, 28].

This approach was firstly reported in 2005 by Leonhardt *et al*. [24]. It was shown that a post-synthesis heating treatment (annealing) of 20 h could allow to achieve a single phase of α-Fe at annealing temperatures of 645 °C in a Ar/H_2 flow. However an unusual oxidation process leading to nanotube decomposition and α-Fe_2O_3 formation was also observed at temperatures of 675 °C. This unusual oxidation process was recently reported also by Boi *et al*. [25] however in this case much lower annealing temperatures of 500 °C were used and the formation of large quantities of α-Fe_2O_3 was observed. Differently, the work reported by Gui *et al*. [26] showed that after 15h of annealing at 645 °C only a fraction of the γ-Fe % could be decomposed into Fe_3C and C, while large quantities of γ-Fe and Fe_3C were still found in the MWCNTs core after the annealing processes. These controversial results suggest therefore that an alternative method that could easily allow at the same time to avoid the nanotube oxidation and guarantee the control of the α-Fe phase is necessary.

In this letter we report a novel chemical vapour deposition approach that through an accurate control of the ferrocene-vapour flow-rate allows to achieve the direct encapsulation of extremely large quantities of α-Fe (95%) without additional heating treatments. The residual 5% of γ-Fe appears to be trapped under the pressure imposed by the MWCNTs walls. In particular through X-ray diffraction (XRD) and Rietveld refinement analyses we show that an exceptional increase in the relative abundance of α-Fe is observed with the increase of the ferrocene/Ar flow rate from 11 ml/min to 120 ml/min. Differently, from 120 ml/min to 150 ml/min an increase of the relative abundance of γ-Fe is observed owing to the shift of the MWCNTs growth area to a zone of the quartz-reactor with an higher temperature. The magnetic properties of the aligned MWCNTs are investigated through vibrating sample magnetometry

Films of aligned MWCNTs were grown on thermally oxidized Si/SiO_2 substrates by sublimation and pyrolysis of 180 mg of ferrocene in an Ar flow setted at 11, 100, 120 and 150 ml/min (each flow rate is used in a different reaction) in a quartz tube reactor (length 1.5 metres) inside a one-zone electrical furnace setted at a

* f.boi@scu.edu.cn

temperature of 990 °C. The reaction time was 15 min. In order to study the phase-changes of the crystals encapsulated inside the MWCNTs during the cooling process, the samples produced with an Ar flow/rate of 11 ml/min were firstly cooled-down at the natural cooling rate of the furnace (0.45 degrees/s) until the temperatures of 929 °C, and 800 °C respectively. A fast cooling method was then used to bring the samples to room temperature. This was achieved by sliding the furnace along a rail system. To study the dependence of the phase-composition of the encapsulated Fe-crystals on the Ar/ferrocene flow rate, three reactions were performed at the flow rates of 100, 120 and 150 ml/min. Also in this case the samples were firstly cooled-down at the natural cooling rate of the furnace until the temperature of 800 °C and then extracted from the reactor after furnace removal. Scanning electron microscopy (SEM) and backscattered electrons investigations of the MWCNTs morphology were performed with a JSM-7500F at 10-20 kV. XRD analyses were performed with a Philips Xpert pro MPD (Cu K-α with $\lambda = 0.154$ nm). The Rietveld refinement method was used to identify and estimate the abundances of the encapsulated Fe-phases [29]. The magnetic measurements were performed at room temperature by employing a vibrating sample magnetometry (VSM) 2.5 Tesla electromagnet East Changing 9060 at 1.3 Tesla. The magnetic measurements are performed at room temperature, so no diamagnetic contribution from the MWCNTs is considered [21, 30, 31].

The morphology of the films of aligned MWCNTs structures was revealed in SEM and back-scattered electron micrographs of the substrates extracted from the reactor after the cooling step. The high aligment of the MWCNTs is shwon in FIG. 1A. FIG. 1B shows the backscattered electron image of randomly oriented MWCNTs removed from the substrate. The encapsulated particles (bright regions) present a typical diameter of 50-100 nm and a length of 100-700 nm.

XRD and Rietveld analyses were then performed in order to study the dependence of the phase composition of the encapsulated Fe-phases on cooling-rate and on the Ar/ferrocene flow rate. In all the XRD measurements the presence of the graphitic MWCNTs walls were revealed by the 002 reflection of graphite with space group P63/mmc (see FIG. 2).

The Rietveld refinement of the XRD diffractogram obtained from the aligned MWCNTs produced with flow rates of 11 ml/min and extracted from the reactor after the cooling stage (cooling rate of 0.45 degrees/s until 929 °C followed by furnace removal) is shown in FIG. 3A. The analyses revealed the presence of an extremely large quantity (89%) of Fe_3C orthorhombic with space group Pnma together with very low quantities of γ-Fe (6%) cubic with space group Fm-3m and α-Fe (5%) cubic with space group Im-3m (see FIG. 3A). In particular the presence of Fe_3C was revealed by the 210, 002, 201, 211, 102, 220, 031, 112, 131, 221 and 122 reflections. The presence of γ-Fe was revealed by the 111 and 200 reflections, while the presence of α-Fe was revealed by the 110 reflection. The XRD and Rietveld refinement analyses of the MWCNTs extracted from the reactor at the temperature of 800 °C (FIG. 3B)revealed only a slight increase of the relative abundance of α-Fe (23%) and a decrease of the relative abundance of Fe_3C (75%) and γ-Fe (2%). These observations confirm the difficulties in controlling the relative abundance of α-Fe inside MWCNTs with the standard cooling methods [6].

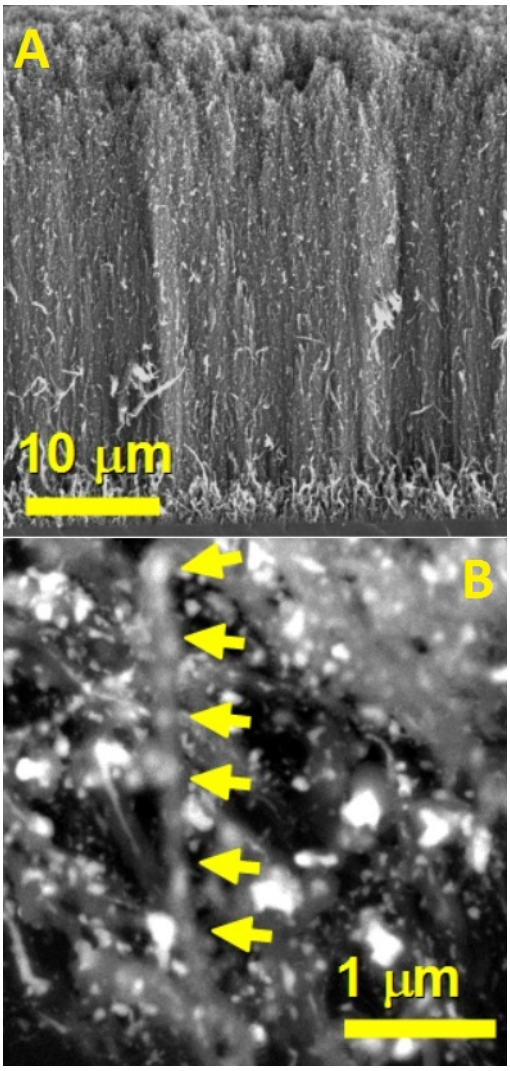

FIG. 1. In A an SEM micrograph shows the cross-sectional morphology of a typical film of aligned MWCNTs. In B the typical diameter of the encapsulated particles is shown by backscattered electrons. The yellow arrows indicate many particles filling a MWCNT along the core.

Differenly when higher Ar/ferrocene flow rates are used with the same cooling conditions (sample extraction at 800 °C) a remarkable change in the XRD diffractogram is observed. The Rietveld refinement of the XRD diffractogram of the MWCNTs produced with a flow rate of 100 ml/min (FIG. 4A) showed a decrease of the relative abundance of Fe_3C (10%) and an increase of the relative abundance of α-Fe to 86%. A relative abundance of 4% was also measured for γ-Fe. By incresing further the flow

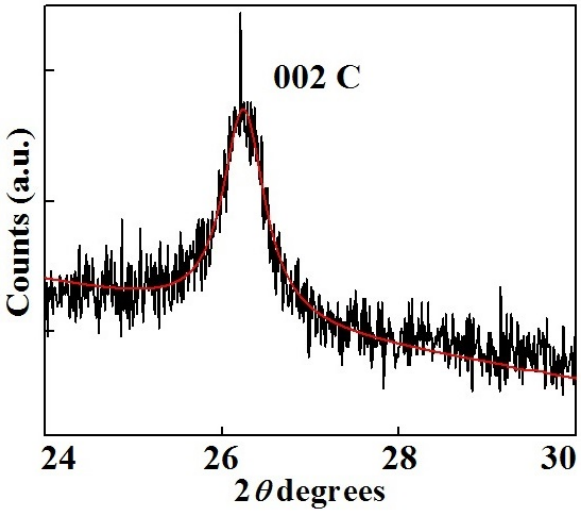

FIG. 2. XRD diffractogram (black line) and Rietveld refinement (red line) of a typical 002 reflection of graphite with space group P63/mmc representing the graphitic MWCNTs walls.

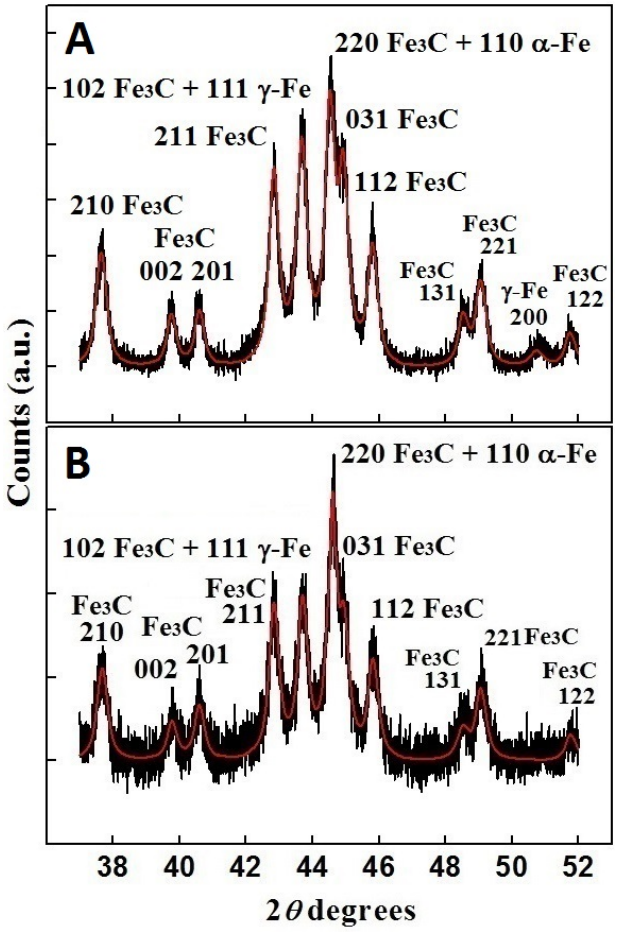

FIG. 3. XRD diffractogram (black line) and Rietveld refinement (red line) of the filled-MWCNTs extracted from the reactor after achieving the temperature of 929 °C (A) and 800 °C (B). Each peak is indicated with the labelled reflection of the corresponding phase.

rate to 120 and 150 ml/min a disappearence of the Fe_3C phase is observed. In particular the Rietveld refinement and XRD diffractogram of the MWCNTs produced with a flow rate of 120 ml/min (FIG. 4B) revealed an increased relative abundance of α-Fe to 95% together with a slight increase of the γ-Fe relative abundance to 5%. A further increase of the relative abundance of γ-Fe to 20% is observed at 150 ml/min (FIG. 4C). These results suggest that an increase of the relative abundance of α-Fe can be obtained by increasing the flow rates to values of 120 ml/min. However owing to the shift of the MWCNTs growth area to higher temperatures with the increase of the flow rate, an increasing relative abundance of γ-Fe is observed at flow rates of 150 ml/min. The remarkable decrease of the relative abundance of Fe_3C from 11 ml/min to 120 ml/min suggests that the Fe-nanoparticles produced at 100-120 ml/min (FIG. 4A-B) are not completely supersaturated but could be covered by a thin layer of Fe_3C that catalyses the MWCNTs growth. This is confirmed also by the XRD diffractogram of FIG. 4B where a small amorphous feature (see black star) is observed.

VSM measurements were then performed at room temperature to compare the magnetic properties of the MWCNTs obtained with a flow rate of 11 ml/min and extracted from the reactor at 800 °C (FIG. 5A) with those of the MWCNTs obtained with a flow rate of 120 ml/min and extracted from the reactor at 800 °C (FIG. 5B) . The hysteresis loop of the MWCNTs obtained with a flow rate of 11 ml/min revealed a saturation magnetization of 57.4 emu/g and an extremely large coercive force of 0.135 T dominated by the magnetocrystalline anisotropy contribution of Fe_3C [4, 12]. Differently an increased saturation magnetization of 85 emu/g and a lower coercivity of 0.08 Tesla due to the shape anisotropy contribution of α-Fe was found in the case of the MWCNTs obtained with a flow rate of 120 ml/min. Interestingly the measured saturation magnetization of 57.4 emu/g for the MWCNTs obtained at 11 ml/min is lower with respect to the estimated saturation magnetization of 177 emu/g for a bulk sample corresponding to (75%) of Fe_3C 23% of α-Fe and 2% of γ-Fe. Furthermore also the saturation magnetization measured in the case of the MWCNTs obtained at 120 ml/min is lower with respect to the estimated saturation magnetization of 209 emu/g for a bulk sample corresponding to 95% of α-Fe and 5% of γ-Fe. The sum of the Fe_3C and α-Fe contributions to the saturation magnetization was estimated by subtracting the weighted average of the saturation magnetization of bulk α-Fe (M_s = 220 emu/g; Curie temperature, T_c= 1043 K) and Fe_3C (M_s= 169 emu/g, T_c = 483 K) [21, 31]. γ-Fe has been reported to be antiferromagnetic below 150K and non magnetic at room temperature, however the presence of an unusual magnetic arrangement of this phase can not be excluded [21, 31]. The origin of the lower saturation magnetization could be also due to the nanocrystalline nature of the sample. The measured values of saturation magne-

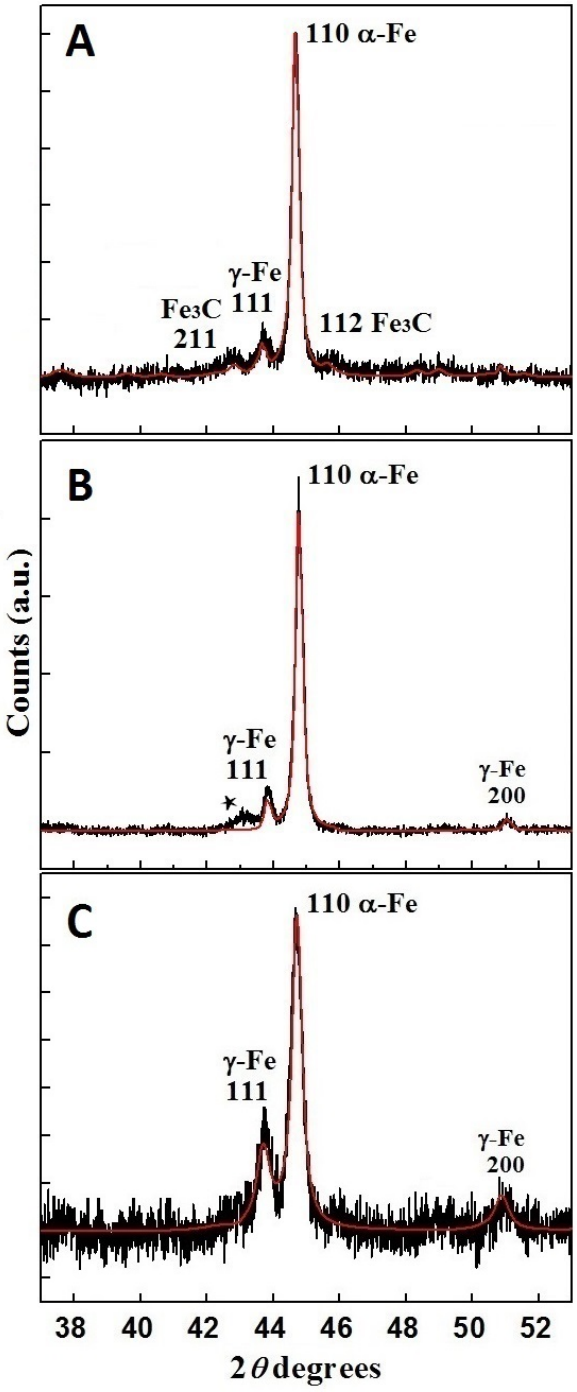

FIG. 4. XRD diffractogram (black line) and Rietveld refinement (red line) of the filled-MWCNTs produced with the Ar flow rates of 100, 120 and 150 ml/min and extracted from the reactor after achieving the cooling-temperature of 800 °C. Each peak is indicated with the labelled reflection of the corresponding phase.

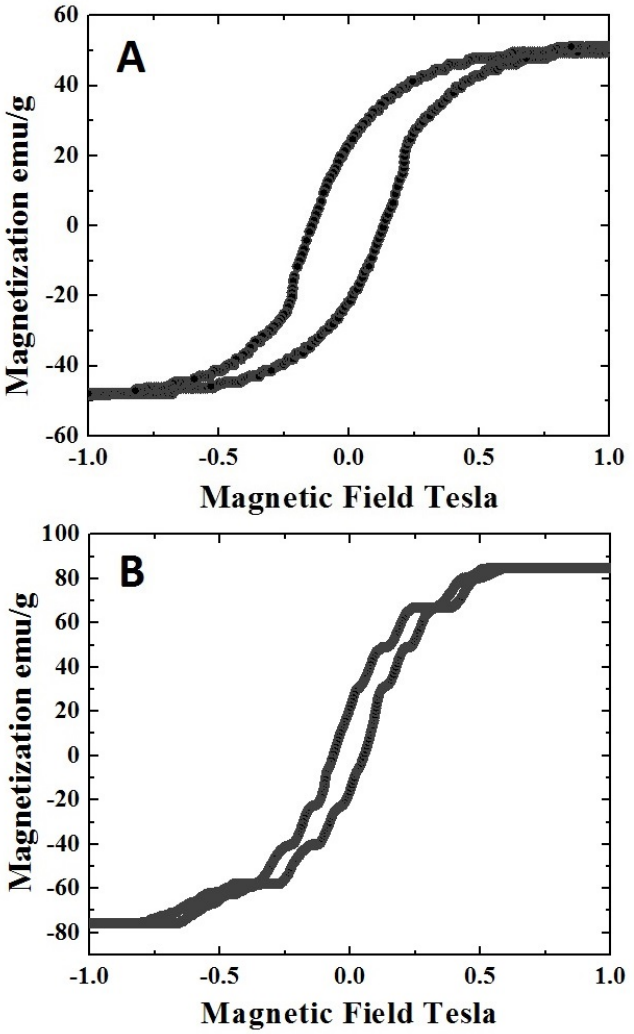

FIG. 5. Hysteresis loops of the MWCNTs obtained with flow rates of 11 ml/min (A) and 120 ml/min (B).

tization are comparable to those previously reported by Leonhardt *et al.* in MWCNTs annealed for 20 h [24]. Furthermore the measured values of coercivities (0.135 Tesla and 0.08 Tesla) are much higher with respect to the coercivities of polycrystalline Fe (1 Oe) and nanocrystalline Fe (23 Oe)[21]. The coercivity measured in the case of MWCNTs obtained at 11 ml/min is much higher with respect to what was measured at room temperature by Prados *et al.* (800 Oe)[13], Karmakar *et al.* (660 Oe)[21], Aaron Morelos-Gomez *et al.*(800 Oe)[11] and Lv *et al.* (500 Oe) [8], but lower with respect to what measured by Hampel *et al.* [7] in the case of MWCNTs filled with mixed Fe-phases owing to the different shape anisotropy contribution.

In conclusion we reported a novel synthesis approach that through an accurate control of the ferrocene-vapour flow-rate allows to achieve the direct encapsulation of extremely large quantities of α-Fe (95%) inside MWCNTs. The MWCNTs produced at flow rates of 120 ml/min (high α-Fe content) possess much higher saturation magnetizations with respect to those produced at flow rates of 11 ml/min (high Fe_3C content). The coercivity decreses with the increase of the α-Fe quantity from 0.135 Tesla (11 ml/min) to 0.08 Tesla (120 ml/min) due to the low shape anisotropy of the encapsulated particles.

I. ACKNOWLEDGMENTS

We acknowledge Prof. Gong Min for his continuous support in this research work. We are also grateful for the financial support from the National Natural Science Foundation of China (Grant Nos. 11004141 and 11174212), the Program for New Century Excellent Talents in University of Ministry of Education of China (Grant No. 11-0351), the Project supported by the Scientific Research Staring Foundation for the Returned Overseas Chinese Scholars, Ministry of Education of China and for financial support from National Natural Science Foundation of China (Grant No. 61307039). We also acknowledge the International Cooperation and Exchange of Science and Technology Project in Sichuan Province under Grant No.2013HH0010.

II. REFERENCES

[1] U. Weissker *et al*. Materials, **3**. 4387, (2010).
[2] A. Leonhardt *et al*. Chemical Vapor Deposition, **12**, 380, (2006).
[3] A. Leonhardt *et al*. Diamond and Related Materials, **12**, 790 (2003).
[4] U. Weissker *et al*. J. Appl. Phys., **106**, 054909 (2009).
[5] F. C. Dillon *et al*. Carbon, **50**, 3674 (2012).
[6] V. Heresanu, *et al*. Journal Physical Chemistry C, **112**, 7371 (2008).
[7] S. Hampel *et al*. Carbon, **44**, 2316 (2006).
[8] L.V. Ruitao, *et al*. Carbon, **47**, 1141(2009).
[9] C. X. Shi,H. T. Cong. Journal of Applied Physics, **104**, 034307 (2008).
[10] H. Terrones *et al*. Solid State Sciences, **8**, 303 (2006).
[11] A. Morelos-Gomez *et al*. Journal of Material Chemistry, **20**, 5906 (2010).
[12] M. U. Lutz *et al*. Journal of Physics: Conference Series, **200**, 072062 (2010).
[13] C. Prados *et al*. Physical Review B, **65**, 113405 (2002).
[14] J.F. Marco *et al*. Hyperfine Interactions, **139**, 535 (2002).
[15] A. K. Schaper *et al*. Journal of Catalysis, **222**, 250 (2004).
[16] F. S. Boi, *et al*. Microscopy and Microanalysis, **19**, 1298 (2013).
[17] D. Golberg *et al*. Acta Materialia, **54**, 2567, (2006).
[18] A.P. Shpak *et al*. Acta Materialia, **55**, 1769, (2007).
[19] S. Groudeva-Zotova *et al*. Journal of Magnetism and Magnetic Materials, **306**, 40, (2006).
[20] F. Geng, H. Cong. Physica B, **382**, 300, (2006).
[21] S. Karmakar, *et al*. Journal of Applied Physics, **97**, 054306 (2005).
[22] C. Muller *et al*. Physica status solidi (a), **203**, 6, 1064 (2006).
[23] C. Muller *et al*. Physica Status Solidi B, **243**, 3091, (2006).
[24] A. Leonhardt *et al*. Journal of Applied Physics, **98**, 074315 (2005).
[25] F. S. Boi, *et al*. Carbon, **64**, 351 (2013).
[26] X. Gui, *et al*. Materials Research Bulletin, **43**, 3441 (2008).
[27] W.D. Callister. *Fundamentals of Materials Science and Engineering,* John Wiley and Sons (2007).
[28] A. Schneider *et al*. Corrosion Science, **44**, 2353, (2002).
[29] C.Hammond. *The basics of Crystallography and Diffraction,* Oxford Science Publications (2009).
[30] V. Likodimos, *et al*. Physical Review B, **68**, 045417 (2003).
[31] F. S. Boi, *et al*. Carbon, **64**, 516 (2013).